













TECH BRIEFS

NATIONAL AERONAUTICS AND SPACE ADMINISTRATION

-  **Technology Focus**
-  **Electronics/Computers**
-  **Software**
-  **Materials**
-  **Mechanics/Machinery**
-  **Manufacturing**
-  **Bio-Medical**
-  **Physical Sciences**
-  **Information Sciences**
-  **Books and Reports**

INTRODUCTION

Tech Briefs are short announcements of innovations originating from research and development activities of the National Aeronautics and Space Administration. They emphasize information considered likely to be transferable across industrial, regional, or disciplinary lines and are issued to encourage commercial application.

Additional Information on NASA Tech Briefs and TSPs

Additional information announced herein may be obtained from the NASA Technical Reports Server: <http://ntrs.nasa.gov>.

Please reference the control numbers appearing at the end of each Tech Brief. Information on NASA's Innovative Partnerships Program (IPP), its documents, and services is available on the World Wide Web at <http://www.ipp.nasa.gov>.

Innovative Partnerships Offices are located at NASA field centers to provide technology-transfer access to industrial users. Inquiries can be made by contacting NASA field centers listed below.

NASA Field Centers and Program Offices

Ames Research Center

David Morse
(650) 604-4724
david.r.morse@nasa.gov

Dryden Flight Research Center

Ron Young
(661) 276-3741
ronald.m.young@nasa.gov

Glenn Research Center

Kimberly A. Dalgleish-Miller
(216) 433-8047
kimberly.a.dalgleish@nasa.gov

Goddard Space Flight Center

Nona Cheeks
(301) 286-5810
nona.k.cheeks@nasa.gov

Jet Propulsion Laboratory

Dan Broderick
(818) 354-1314
daniel.f.broderick@jpl.nasa.gov

Johnson Space Center

John E. James
(281) 483-3809
john.e.james@nasa.gov

Kennedy Space Center

David R. Makufka
(321) 867-6227
david.r.makufka@nasa.gov

Langley Research Center

Michelle Ferebee
(757) 864-5617
michelle.t.ferebee@nasa.gov

Marshall Space Flight Center

Terry L. Taylor
(256) 544-5916
terry.taylor@nasa.gov

Stennis Space Center

Ramona Travis
(228) 688-3832
ramona.e.travis@ssc.nasa.gov

NASA Headquarters

Daniel Lockney,
Technology Transfer Program Executive
(202) 358-2037
daniel.p.lockney@nasa.gov

Small Business Innovation Research (SBIR) & Small Business Technology Transfer (STTR) Programs

Rich Leshner, Program Executive
(202) 358-4920
rleshner@nasa.gov



TECH BRIEFS

NATIONAL AERONAUTICS AND SPACE ADMINISTRATION



5 Technology Focus: Data Acquisition

- 5 Remote Data Access with IDL
- 5 Data Compression Algorithm Architecture for Large Depth-of-Field Particle Image Velocimeters
- 5 Vectorized Rebinning Algorithm for Fast Data Down-Sampling
- 6 Display Provides Pilots with Real-Time Sonic-Boom Information
- 6 Onboard Algorithms for Data Prioritization and Summarization of Aerial Imagery
- 7 Monitoring and Acquisition Real-time System (MARS)



9 Electronics/Computers

- 9 Analog Signal Correlating Using an Analog-Based Signal Conditioning Front End
- 9 Micro-Textured Black Silicon Wick for Silicon Heat Pipe Array
- 10 Robust Multivariable Optimization and Performance Simulation for ASIC Design



13 Manufacturing & Prototyping

- 13 Castable Amorphous Metal Mirrors and Mirror Assemblies



15 Mechanics/Machinery

- 15 Sandwich Core Heat-Pipe Radiator for Power and Propulsion Systems
- 16 Apparatus for Pumping a Fluid
- 17 Cobra Fiber-Optic Positioner Upgrade



19 Materials & Coatings

- 19 Improved Wide Operating Temperature Range of Li-Ion Cells
- 19 Non-Toxic, Non-Flammable, -80 °C Phase Change Materials
- 20 Soft-Bake Purification of SWCNTs Produced by Pulsed Laser Vaporization



23 Bio-Medical

- 23 Improved Cell Culture Method for Growing Contracting Skeletal Muscle Models
- 24 Hand-Based Biometric Analysis
- 24 The Next Generation of Cold Immersion Dry Suit Design Evolution for Hypothermia Prevention



27 Software

- 27 Integrated Lunar Information Architecture for Decision Support Version 3.0 (ILIADS 3.0)
- 27 Relay Forward-Link File Management Services (MaROS Phase 2)
- 27 Two Mechanisms to Avoid Control Conflicts Resulting from Uncoordinated Intent
- 28 XTCE GOVSAT Tool Suite 1.0



29 Information Technology

- 29 Determining Temperature Differential to Prevent Hardware Cross-Contamination in a Vacuum Chamber
- 29 SequenCL: Automated Parallel Algorithms Derived from CSP-NT Computational Laws
- 30 Remote Data Exploration with the Interactive Data Language (IDL)
- 30 Mixture-Tuned, Clutter Matched Filter for Remote Detection of Subpixel Spectral Signals



31 Physical Sciences

- 31 Partitioned-Interval Quantum Optical Communications Receiver
- 32 Practical UAV Optical Sensor Bench With Minimal Adjustability

This document was prepared under the sponsorship of the National Aeronautics and Space Administration. Neither the United States Government nor any person acting on behalf of the United States Government assumes any liability resulting from the use of the information contained in this document, or warrants that such use will be free from privately owned rights.



Remote Data Access with IDL

Goddard Space Flight Center, Greenbelt, Maryland

A tool based on IDL (Interactive Data Language) and DAP (Data Access Protocol) has been developed for user-friendly remote data access. A difficulty for many NASA researchers using IDL is that often the data to analyze are located remotely and are too large to transfer for local analysis. Researchers have developed a protocol for accessing remote data, DAP, which is used for both SOHO and STEREO data sets. Server-side side

analysis via IDL routine is available through DAP.

The tools allow normal DAP users to run IDL scripts on their data remotely via DAP. This powerful, user-friendly interface to DAP for IDL improved OPeNDAP bindings that fixed bugs in existing functionality, created a GUI client to explore data sets served with DAP, developed a pure IDL DAP implementation that provided complete DAP capabilities

along with a simple installation, improved network capabilities for GDL (the open source IDL alternative) and older versions of IDL, and modified the OPeNDAP Hyrax DAP server to process data on the server-side via a syntax in the DAP request.

This work was done by Michael Galloy of Tech-X Corporation for Goddard Space Flight Center. Further information is contained in a TSP (see page 1). GSC-16253-1

Data Compression Algorithm Architecture for Large Depth-of-Field Particle Image Velocimeters

Goddard Space Flight Center, Greenbelt, Maryland

A large depth-of-field particle image velocimeter (PIV) is designed to characterize dynamic dust environments on planetary surfaces. This instrument detects lofted dust particles, and senses the number of particles per unit volume, measuring their sizes, velocities (both speed and direction), and shape factors when the particles are large. To measure these particle characteristics in-flight, the instrument gathers two-dimensional image data at a high frame rate, typically >4,000 Hz, generating large amounts of data for every second of operation, approximately 6 GB/s.

To characterize a planetary dust environment that is dynamic, the instrument would have to operate for at least several minutes during an observation period, easily producing more than a terabyte of data per observation. Given current technology, this amount of data would be very difficult to store onboard a spacecraft, and downlink to Earth. Since 2007, innovators have been developing an autonomous image analysis algorithm architecture for the PIV instrument to greatly reduce the amount of data that it has to store and downlink. The algorithm analyzes PIV images and automatically reduces the

image information down to only the particle measurement data that is of interest, reducing the amount of data that is handled by more than 10^3 . The state of development for this innovation is now fairly mature, with a functional algorithm architecture, along with several key pieces of algorithm logic, that has been proven through field test data acquired with a proof-of-concept PIV instrument.

This work was done by Brent Bos, Nargess Memarsadeghi, Semion Kizhner, and Scott Antonille of Goddard Space Flight Center. Further information is contained in a TSP (see page 1). GSC-15960-1

Vectorized Rebinning Algorithm for Fast Data Down-Sampling

Applications include image processing, filter design, and anti-aliasing techniques.

Goddard Space Flight Center, Greenbelt, Maryland

A vectorized rebinning (down-sampling) algorithm, applicable to N-dimensional data sets, has been developed that offers a significant reduction in computer run time when compared to conventional rebinning algorithms. For clarity, a two-dimensional version of the algorithm is discussed to illustrate some specific details of the algorithm content, and using the language of image pro-

cessing, 2D data will be referred to as “images,” and each value in an image as a “pixel.” The new approach is fully vectorized, i.e., the down-sampling procedure is done as a single step over all image rows, and then as a single step over all image columns.

Data rebinning (or down-sampling) is a procedure that uses a discretely sampled N-dimensional data set to create a

representation of the same data, but with fewer discrete samples. Such data down-sampling is fundamental to digital signal processing, e.g., for data compression applications. Additional applications include image processing, filter design, and anti-aliasing techniques. Data rebinning is a computationally intensive procedure and thus the goal in this technology development is a more efficient algorithm

with reduced run times, as compared to existing rebinning approaches. This approach is able to take advantage of vectorized instructions such as Single Instruction Multiple Data (SIMD), to perform the rebinning operation.

The algorithm completely vectorizes the data rebinning operation, in the sense that a “single” arithmetic operation is applied simultaneously to multiply distinct data sets and is executed with the approximate run time of that operation applied to a single data set. For lower-level computer languages, such as C or assembly, vectorized operations can

be implemented using central processing unit (CPU) single-instruction, multiple-data (SIMD) capabilities, such as streaming SIMD Extensions 3 (SSE3) on x86 computer architecture or AltiVec on PowerPC processors. Thus, although the algorithm has been implemented using MATLAB, it is not fundamentally tied to MATLAB, and can be implemented using other programming languages.

The vectorized data rebinning (downsampling) procedure offers a reduced run time when compared with standard rebinning algorithms. In general, algorithms are often optimized by trading

decreased run time for increased memory, where the latter is needed for storing additional code, pre-computed results, or other ancillary data. However, the vectorized rebinning approach does not have increased memory requirements compared with conventional approaches. The underlying fundamental advantage to this technology is the utilization of vectorized instructions for the rebinning operation.

This work was done by Bruce Dean, David Aronstein, and Jeffrey Smith of Goddard Space Flight Center. Further information is contained in a TSP (see page 1). GSC-15949-1

Display Provides Pilots with Real-Time Sonic-Boom Information

The impact of sonic booms can be controlled over populated areas.

Dryden Flight Research Center, Edwards, California

Supersonic aircraft generate shock waves that move outward and extend to the ground. As a cone of pressurized air spreads across the landscape along the flight path, it creates a continuous sonic boom along the flight track. Several factors can influence sonic booms: weight, size, and shape of the aircraft; its altitude and flight path; and weather and atmospheric conditions. This technology allows pilots to control the impact of sonic booms.

A software system displays the location and intensity of shock waves caused by supersonic aircraft. This technology can be integrated into cockpits or flight control rooms to help pilots minimize sonic-boom impact in populated areas. The system processes vehicle and flight parameters as well as data regarding cur-

rent atmospheric conditions. The display provides real-time information regarding sonic boom location and intensity, enabling pilots to make the necessary flight adjustments to control the timing and location of sonic booms. This technology can be used on current-generation supersonic aircraft, which generate loud sonic booms, as well as future-generation, low-boom aircraft, anticipated to be quiet enough for populated areas.

When fully deployed in real time, the display will leverage existing tools developed and enhanced by the U.S. Air Force and NASA to predict sonic boom parameters. The prediction data will be integrated with a real-time, local-area, moving-map display that is capable of displaying the aircraft’s current sonic

boom footprint at all times. The pilot will be able to choose from a menu of pre-programmed maneuvers such as accelerations, turns, or pushovers, and the predicted sonic boom footprint for that maneuver appears on the map. After fully developed and implemented, this will allow the pilot to select or modify parameters to either avoid generating a sonic boom or to place the sonic boom in a specific location. The system may also provide pilots with guidance on how to execute the chosen maneuver.

This technology will enable supersonic commercial flight without disturbing population centers on the ground.

This work was done by Ed Haering of Dryden Flight Research Center and Ken Plotkin of Wyle. Further information is contained in a TSP (see page 1). DRC-008-001

Onboard Algorithms for Data Prioritization and Summarization of Aerial Imagery

Clustering/machine learning methods are used to structure data for prioritization, mapping, and downlinking.

NASA’s Jet Propulsion Laboratory, Pasadena, California

Many current and future NASA missions are capable of collecting enormous amounts of data, of which only a small portion can be transmitted to Earth. Communications are limited due to distance, visibility constraints, and competing mission downlinks. Long missions and high-resolution, multispectral imag-

ing devices easily produce data exceeding the available bandwidth. To address this situation, computationally efficient algorithms were developed for analyzing science imagery onboard the spacecraft. These algorithms autonomously cluster the data into classes of similar imagery, enabling selective downlink of represen-

tatives of each class, and a map classifying the terrain imaged rather than the full dataset, reducing the volume of the downlinked data. A range of approaches was examined, including k-means clustering using image features based on color, texture, temporal, and spatial arrangement.

Several unique challenges influenced design decisions for automatic image analysis. First, onboard processing is limited in spaceflight applications. Avionics computers must satisfy strict radiation and energy constraints, and their resources are shared between continuous autonomous control and data processing. Computational constraints mandate a simple approach to image analysis in which statistical properties of the image serve as proxies for the actual content.

A major challenge is the diversity of surface features an aerobot might encounter. An aerobot would be in constant motion but difficult to control due to unpredictable atmospheric currents. It would be difficult to schedule image targets in advance or to anticipate the features of interest that will appear. This

favors an “unsupervised” approach that makes few assumptions about image content but instead discovers interesting and representative samples based on the intrinsic properties of the data. Clustering is one common unsupervised approach; it classifies a dataset into discrete categories of items with similar properties.

Image features can be considered to fall into one of four groups, or themes, based on the properties they describe. These are color, edge, frequency, and time. The edge and frequency features correlate with image texture, color captures basic color statistics, and time describes the temporal order in which the images were collected.

The main feature of this innovation is the use of clustering/machine learning

methods to structure data for prioritization, mapping, and downlink. The effectiveness of clustering rests on the quality of the feature vectors describing each set of data. Features that are redundant, or have little variance, will reduce the effectiveness of clustering. Dimensionality reduction techniques such as principal component analysis (PCA) can transform a high-dimensional feature space into a lower-dimensional space where the new, uncorrelated features have heightened variance. Ideal clusterings contain compact clusters that are spread far apart from one another.

This work was done by Steve A. Chien, David Hayden, David R. Thompson, and Rebecca Castano of Caltech for NASA’s Jet Propulsion Laboratory. For more information, contact iaoffice@jpl.nasa.gov. NPO-47534

Monitoring and Acquisition Real-time System (MARS)

Marshall Space Flight Center, Alabama

MARS is a graphical user interface (GUI) written in MATLAB and Java, allowing the user to configure and control the Scalable Parallel Architecture for Real-Time Acquisition and Analysis (SPARTAA) data acquisition system. SPARTAA not only acquires data, but also allows for complex algorithms to be applied to the acquired data in real time. The MARS client allows the user to set up and configure all settings regarding the data channels attached to the system, as well as have complete control over starting and stopping data acquisition. It provides a unique “Test” programming environment, allowing the user to create tests consisting of a series of alarms, each of which contains any number of data channels. Each alarm is configured with a particular algorithm, determining the type of processing that will be applied on each data channel and tested against a

defined threshold. Tests can be uploaded to SPARTAA, thereby teaching it how to process the data.

MARS was developed as a front-end GUI for setup, control, and plotting of data from SPARTAA. The system was designed to monitor spectral components in real time from instrumentation located on high-speed rotational hardware (primarily high-pressure turbopumps), and to issue cut commands to a facility if preset levels were violated. However, the system is not limited to rotational hardware, and can be used to monitor any level of frequency information from a myriad of instrumented test hardware. The control software allows the user to configure the system easily to support testing of various configurations with multiple alarms, voting logic, and sensor validation,

The uniqueness of MARS is in its capability to be adaptable easily to many

test configurations. Test hardware measurement limits (i.e. vibration, pressure, temperature, etc.) can be predetermined, and MARS can be used to set up and support quickly any test configuration. Multiple alarms with various timings can be configured within minutes, as opposed to previous software modifications. MARS sends and receives protocols via TCP/IP, which allows for quick integration into almost any test environment. The use of MATLAB and Java as the programming languages allows for developers to integrate the software across multiple operating platforms.

This work was done by Corbin Holland of Marshall Space Flight Center. For more information, contact Sammy Nabors, MSFC Commercialization Assistance Lead, at sammy.a.nabors@nasa.gov. Refer to MFS-32905-1.



Analog Signal Correlating Using an Analog-Based Signal Conditioning Front End

Converting a signal into a bit stream simplifies the correlation function calculation.

John H. Glenn Research Center, Cleveland, Ohio

This innovation is capable of correlating two analog signals by using an analog-based signal conditioning front end to hard-limit the analog signals through adaptive thresholding into a binary bit stream, then performing the correlation using a Hamming “similarity” calculator function embedded in a one-bit digital correlator (OBDC). By converting the analog signal into a bit stream, the calculation of the correlation function is simplified, and less hardware resources are needed. This binary representation allows the hardware to move from a DSP where instructions are performed serially, into digital logic where calculations can be performed in parallel, greatly speeding up calculations.

Each of two analog signals (channels A and B) is converted to a digital bit stream by phase correcting it and comparing it to an average of itself at a sampling clock rate f . The hard-limited conversions of A and B are bitwise compared to measure the level of similarity between the two by the OBDC.

This similarity measurement X is equal to the maximum possible Hamming distance (N bits in disagreement) minus the measured number of bits in disagreement.

The OBDC functions are embedded into a field programmable gate array (FPGA). The OBDC is made up of two shift registers containing the current sample values (of length N) from each of the two input channels (A and B). During each sample clock, a new sample from each A and B input is clocked into the input linear shift register for each respective channel; this input shifts the current values in the linear shift register. The oldest ($N + 1$ sample clocks ago) sample is clocked out of the register. Once the inputs have been clocked in, the correlation routine can start. This rising edge of the sample clock also clears the max correlation value, the best correlation index, and the shift counter registers, initializing the correlator.

When the two registers match exactly, or are correlated, the X value will equal

N . Once the correlation value has been calculated, this result is forwarded to compare with the max correlation value register. If the X value is greater than the current max correlation value, then the max correlation value becomes X , and the shift counter register is latched and put into the best correlation index register, providing the index of the current best correlation.

This index is the number of sample clock periods difference between the two input signals and thus, for sample clock rate f , indicates the delay between the signals A and B.

This work was done by Norman Prokop and Michael Krasowski of Glenn Research Center. Further information is contained in a TSP (see page 1).

Inquiries concerning rights for the commercial use of this invention should be addressed to NASA Glenn Research Center, Innovative Partnerships Office, Attn: Steven Fedor, Mail Stop 4-8, 21000 Brookpark Road, Cleveland, Ohio 44135. Refer to LEW-18902-1.

Micro-Textured Black Silicon Wick for Silicon Heat Pipe Array

This technology can be used for microprocessors, power switching circuits, and diode lasers in high-power electronics.

NASA's Jet Propulsion Laboratory, Pasadena, California

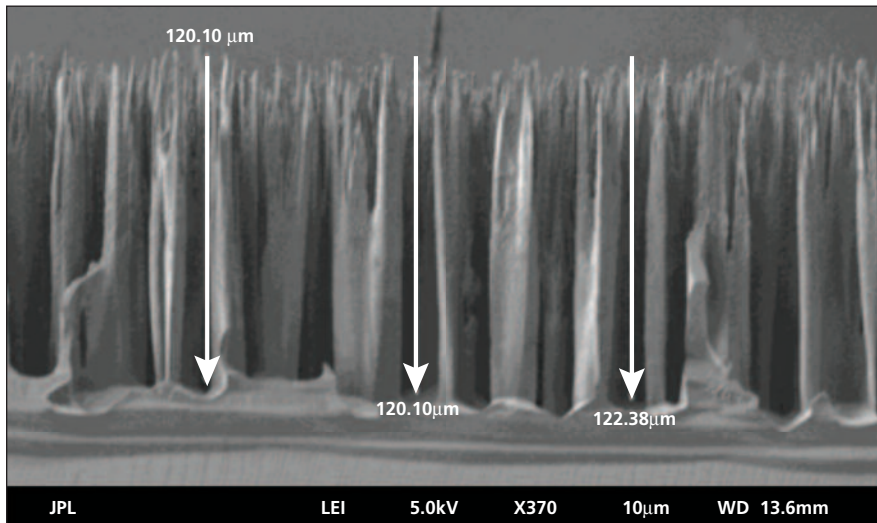
Planar, semiconductor heat arrays have been previously proposed and developed; however, this design makes use of a novel, microscale black silicon wick structure that provides increased capillary pumping pressure of the internal working fluid, resulting in increased effective thermal conductivity of the device, and also enables operation of the device in any orientation with respect to the gravity vector.

In a heat pipe, the efficiency of thermal transfer from the case to the working fluid is directly proportional to the surface area of the wick in contact with

the fluid. Also, the primary failure mechanism for heat pipes operating within the temperature range of interest is inadequate capillary pressure for the return of fluid from the condenser to the wick. This is also what makes the operation of heat pipes orientation-sensitive. Thus, the two primary requirements for a good wick design are a large surface area and high capillary pressure. Surface area can be maximized through nanomachined surface roughening. Capillary pressure is largely driven by the working fluid and wick structure.

The proposed nanostructure wick has characteristic dimensions on the order of tens of microns, which promotes menisci of very small radii. This results in the possibility of enormous pumping potential due to the inverse proportionality with radius. Wetting, which also enhances capillary pumping, can be maximized through growth of an oxide layer or material deposition (e.g. TiO_2) to create a superhydrophilic surface.

In addition, the wick fabrication technique produces nanostructure forests that



SEM photo showing black silicon formed by ICP cryo etching.

are planar, and can take advantage of 2D heat spreading over a surface vs. state-of-the-art 1D heat transport associated with heat pipes. The combined result of these

benefits promises to be a two-phase heat transfer device, which is very insensitive to a gravity field. Although liquid pressure drops may be relatively large depending

on the nanostructure density, the overall device dimensions of $\approx 7 \times 7$ cm are expected to be well within the overall capillary limit. The novel aspects of the currently proposed effort include the use of the phenomenon of superhydrophilicity in a heat pipe, and the wick geometry, control of the nanotip height density, and the method for creating this nanotip texture. A cryo-etch inductively coupled plasma is used to make the nanotips, enabling the cost-effective, mask-free formation of a uniform black silicon surface over a large area, with nanotip heights exceeding 100 microns. Unlike nanotextured surfaces formed by the growth or deposition of materials (e.g. carbon nanotubes), the resulting formations are robust and compatible with liquid processes.

This work was done by Karl Y. Yee, Eric T. Sunada, Gani B. Ganapathi, Harish Manohara, and Andrew Homyk of Caltech, and Mauro Prina of SpaceX for NASA's Jet Propulsion Laboratory. Further information is contained in a TSP (see page 1). NPO-47299

Robust Multivariable Optimization and Performance Simulation for ASIC Design

Systematic method automates the simulation and optimization of circuits.

Goddard Space Flight Center, Greenbelt, Maryland

Application-specific-integrated-circuit (ASIC) design for space applications involves multiple challenges of maximizing performance, minimizing power, and ensuring reliable operation in extreme environments. This is a complex multidimensional optimization problem, which must be solved early in the development cycle of a system due to the time required for testing and qualification severely limiting opportunities to modify and iterate. Manual design techniques, which generally involve simulation at one or a small number of corners with a very limited set of simultaneously variable parameters in order to make the problem tractable, are inefficient and not guaranteed to achieve the best possible results within the performance envelope defined by the process and environmental requirements. What is required is a means to automate design parameter variation, allow the designer to specify operational constraints and performance goals, and to analyze the results in a way that facilitates identifying the tradeoffs defining

the performance envelope over the full set of process and environmental corner cases.

The system developed by the Mixed Signal ASIC Group (MSAG) at the Goddard Space Flight Center is implemented as a framework of software modules, templates, and function libraries. It integrates CAD tools and a mathematical computing environment, and can be customized for new circuit designs with only a modest amount of effort as most common tasks are already encapsulated. Customization is required for simulation test benches to determine performance metrics and for cost function computation. Templates provide a starting point for both, while toolbox functions minimize the code required. Once a test bench has been coded to optimize a particular circuit, it is also used to verify the final design. The combination of test bench and cost function can then serve as a template for similar circuits or be re-used to migrate the design to different processes by re-running it with the new process-

specific device models. The system has been used in the design of time- to-digital converters for laser ranging and time-of-flight mass spectrometry to optimize analog, mixed signal and digital circuits such as charge sensitive amplifiers, comparators, delay elements, radiation tolerant dual interlocked (DICE) flip-flops, and two of three voter gates.

The overall structure of the framework consists of two processes running independently and communicating with each other via a data and handshaking file interface. The master optimization process contains the multivariable optimization algorithm and performs top level analysis of results to select the best solution. It is currently implemented in the Scilab open source environment for numerical computation. This environment is supported on multiple platforms, is well suited to performing numerical analysis and data visualization, and has the advantage of being free to use. Cost can be a significant consideration since multiple copies of the environment may need to run for hours or even days at a time.

The simulation process acts as a slave process, simulating the circuit being optimized using the parameters specified by the optimization process and re-

turning the results. It is currently implemented in the Skill programming language running in the Cadence environment.

This work was done by Jeffrey DuMonthier and George Suarez of Goddard Space Flight Center. Further information is contained in a TSP (see page 1). GSC-16185-1



Castable Amorphous Metal Mirrors and Mirror Assemblies

Commercial applications include optics for spacecraft and satellites, mirror components for telescopes, and mirrors for lasers, sensing, and solar energy collection.

NASA's Jet Propulsion Laboratory, Pasadena, California

The use of mirror assemblies is commonplace in the aerospace industry, as most satellites and spacecraft contain optics. The fabrication of these mirrors is extremely complex due to the nature of their intended use, which includes telescope lenses, camera optics, or laser mirrors. Some of the common requirements of spacecraft mirrors are that they have the correct optical curvature to some defined tolerance, they have low surface roughness, they have high reflectivity, and they are rigid (either against thermal expansion or flexing).

Typical spacecraft mirrors are either fabricated by coating oxide glass with a metal layer or by machining, polishing, and coating metal mirrors. Oxide glass exhibits a low coefficient of thermal expansion (CTE) and can be made very smooth but is also dense, brittle, and difficult to bond to mirror-mounts. Metal mirrors are tough and light, but must typically be diamond-turned to achieve

an optical surface and exhibit very high CTEs. Moreover, support structures, such as isogrids, flexures, or tabs, must be machined out of large blocks of metal or bolted on separately to the mirror. The use of different CTE materials in a mirror and mirror assembly causes misalignment and thermal cracking.

A revolutionary way to produce a mirror and mirror assembly is to cast the entire part at once from a metal alloy that combines all of the desired features into the final part: optical smoothness, curvature, flexures, tabs, isogrids, low CTE, and toughness. In this work, it has been demonstrated that castable mirrors are possible using bulk metallic glasses (BMGs, also called amorphous metals) and BMG matrix composites (BMGMCs). These novel alloys have all of the desired mechanical and thermal properties to fabricate an entire mirror assembly without machining, bonding, brazing, welding, or epoxy. BMGs are multi-component metal alloys that have been cooled in such a manner as to avoid crystallization, leading to an amorphous (non-crystalline) microstructure. This lack of crystal structure, and the fact that these alloys are glasses, leads to a wide assortment of mechanical and thermal properties that are unlike those observed in crystalline metals. Among these are high yield strength, carbide-like hardness, low melting temperatures (making them castable like aluminum), a thermoplastic processing region (for improving smoothness), low stiffness, high strength-to-weight ratios, relatively low CTE, density similar to titanium alloys, high elasticity, and ultra-smooth cast parts (as low as 0.2-nm surface roughness has been demonstrated in cast BMGs). BMGMCs are composite alloys that consist of a BMG matrix with crystalline dendrites embedded throughout. BMGMCs are used to overcome the typically brittle failure observed in monolithic BMGs by adding a soft phase that arrests the formation of cracks in the BMG matrix. In some cases, BMGMCs offer superior castabil-

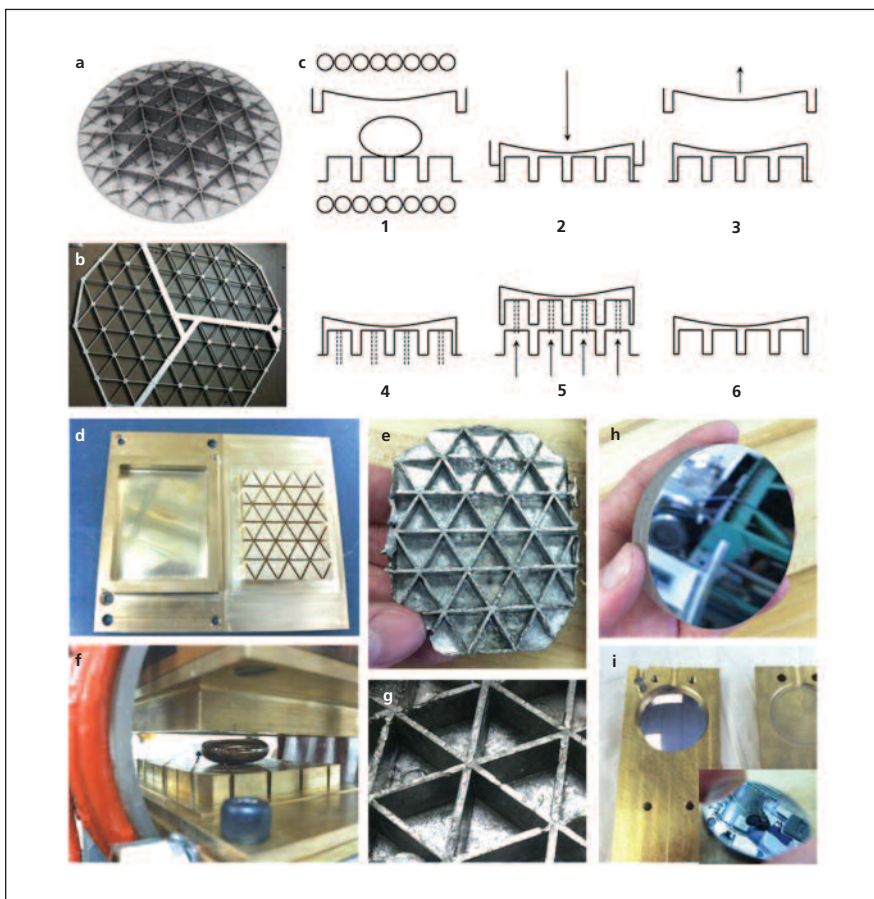


Figure (a) Example of an Isogrid Mirror Backing machined from a solid block of metal. (b) An aluminum isogrid machined from a solid plate. (c) The processing steps necessary to fabricate an amorphous metal mirror and isogrid in a single step. An ingot of amorphous metal or composite is heated using radio frequency heating while sitting on water-cooled molds. The liquid is forged into the mold and cools into a glass, which allows it to be ejected from the mold without sticking. With sufficient casting pressure, the isogrid and the mirror surface can be fabricated in one step. (d-g) The water cooled brass molds used to make the mirror, the isogrid, and the part after being ejected from the mold. (h) Example of a mirror assembly with isogrid backing all made from an amorphous metal. (i) A mirror polished steel mold with curvature acts as the template for casting a perfect metallic glass mirror (shown in the inset).

ity, toughness, and fatigue resistance, if not as good a surface finish as BMGs.

As shown in the figure, this work has demonstrated that BMGs and BMGMCs can be cast into prototype mirrors and mirror assemblies without difficulty. Optical curvature, ultra-smooth surfaces, and isogrids have all been demonstrated using this technology. A commercially manufactured version of these alloys would exhibit a smooth surface directly off a mold, any desired curvature or size, and all flexures, tabs, and isogrids built into the final part. This would eliminate the need for machining, would reduce the CTE mismatch in the part by making it all from the same material and removing connections, would eliminate fatigue or stress cracking, and would be low-cost (since thousands could be fabricated using a single mold).

The novelty of the current work is that tremendous cost and time savings can be achieved by casting the mirror assembly into a net or near-net shape using a metal alloy. This work suggests that mirror assemblies can be cast or fabricated using BMGs or BMGMCs where the entire part can be made using a simple and repeatable processing procedure to form the mirror into the same shape as

the conventional mirror assembly, but without the need for machining from a billet. This idea is novel for a number of reasons, including that conventional metal alloys cannot be cast into net shapes without great expense, and this unique class of metal alloys has the ability to be cast, repeatedly, into reusable molds to net shapes and yet still have the hardness and toughness to satisfy the requirements for being used as a mirror assembly. Unlike crystalline metals, BMGMCs also have unique joining properties that allow them to be welded together into solid structures without heat-affected zones, which removes bonding, bolting, and brazing from assembly.

This work has the potential to make a broad impact in the way that mirror assemblies are fabricated for spacecraft, satellites, and terrestrial optics. Since most NASA spacecraft and satellites require optics, the current invention may provide a path for creating high-performance mirrors while greatly reducing their cost. Moreover, the invention may result in an assembly-line-type process for fabricating mirror assemblies that will reduce the cost of terrestrial optics, such as mirrors and telescopes.

The last technique demonstrated is a localized surface treatment as a way to take a near-net shape and turn it into a mirror finish. In this technique, the BMG mirror assembly is fabricated through one of the strategies described above, but the mirror finish is left in a rough state. The mirror assembly is then subjected to a surface treatment that produces an optical mirror surface without machining, grinding, or polishing.

This work was done by Douglas C. Hoffmann, Gregory L. Davis, Gregory S. Agnes, and Andrew A. Shapiro of Caltech for NASA's Jet Propulsion Laboratory. For more information, contact iaoffice@jpl.nasa.gov.

In accordance with Public Law 96-517, the contractor has elected to retain title to this invention. Inquiries concerning rights for its commercial use should be addressed to:

*Innovative Technology Assets Management
JPL*

*Mail Stop 321-123
4800 Oak Grove Drive
Pasadena, CA 91109-8099*

E-mail: iaoffice@jpl.nasa.gov

Refer to NPO-48438, volume, and number of this NASA Tech Briefs issue, and the page number.



Sandwich Core Heat-Pipe Radiator for Power and Propulsion Systems

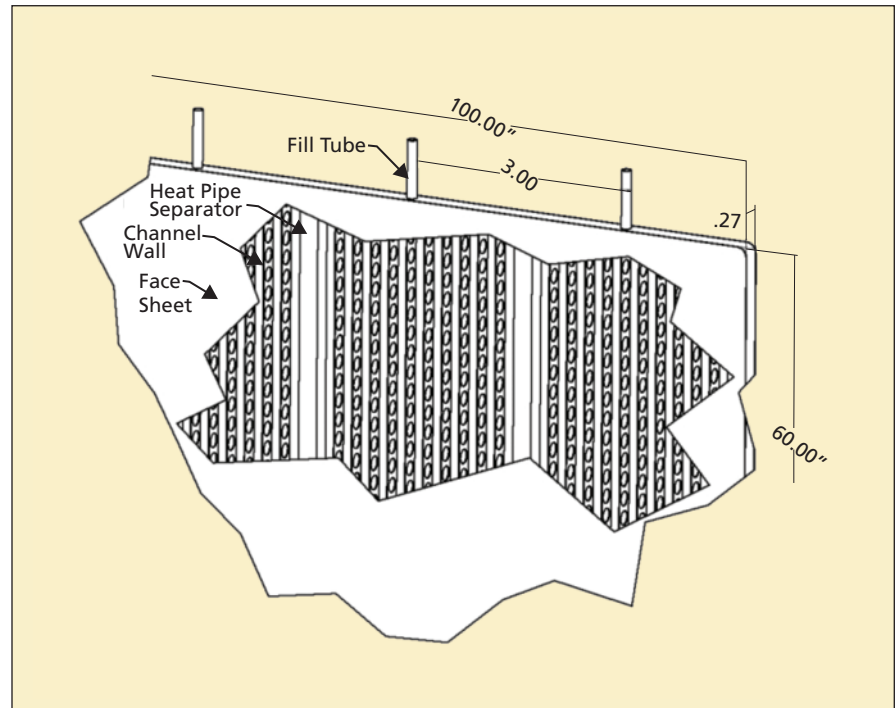
This technology has a potential use for residential or commercial radiant heating systems using lower-cost materials of construction.

John H. Glenn Research Center, Cleveland, Ohio

Next-generation heat-pipe radiator technologies are being developed at the NASA Glenn Research Center to provide advancements in heat-rejection systems for space power and propulsion systems. All spacecraft power and propulsion systems require their waste heat to be rejected to space in order to function at their desired design conditions. The thermal efficiency of these heat-rejection systems, balanced with structural requirements, directly affect the total mass of the system.

In testing space radiators for nuclear power systems, it was found that current technology had significant thermal losses due to the long chains of thermal resistance, stemming from multiple materials, their respective bonds, and physical geometries. Tubular heat pipes connected to flat fins, typically made of different materials, have traditionally been thought of as the best way to drive down radiator system mass. Dissimilar materials inherently had coefficient of thermal expansion mismatches, which created complex designs and additional mass.

Combining structural and thermal components of a heat-pipe radiator into a unique design may produce advantages to both heat transfer characteristics and structural integrity. The Sandwich Core Heat Pipe (SCHP) technology being developed at the Glenn Research Center addresses this by using thin titanium sheets in a unique structural configuration to make a highly efficient rectangular heat-pipe array that can be used as a thermal-control radiator. The concept is the first of its kind to combine heat pipes, radiator, and structural components into one system using a single material of construction. Although numerous concepts are under development, the basic design allows the internal sandwich core structure to double as the heat pipe vapor space, allowing the radiator facesheet to reach near-vapor temperatures without the



The **Titanium Radiator** incorporates multiple rectangular heat pipe channels, and an enclosed pressure boundary using a single facesheet, all from the same material. Each channel can be shared with neighboring channels to create a multi-channel heat pipe.

losses associated with a conduction fin, common to current state-of-the-art technology. This “no fin” feature reduces the overall temperature drop associated with current heat-pipe radiator designs and ultimately reduces unwanted mass through improved thermal efficiency. Additionally, the configuration of the internal core using thin metal construction provides rigidity as well as a reduction in mass over current technologies. The combination of the reduced mass and increased thermal efficiency are appealing to power and propulsion designers needing improved performance.

Although the materials of choice for current fission power systems are titanium and water, many different heat-pipe configurations could be developed using other metals and working

fluids. The significance of this approach is that the same basic design could be used for multiple temperature ranges, dependent only on the material of construction, working fluid thermophysical properties, and the material/fluid compatibility.

Terrestrially, this technology could be used for thermal control of structural systems. One potential use is radiant heating systems for residential and commercial applications. The thin cross section and efficient heat transportability could easily be applied to flooring and wall structures that could evenly heat large surface areas. Using this heat-pipe technology, the evaporator of the radiators could be heated using any household heat source (electric, gas, etc.), which would vaporize the internal working fluid and carry the

heat to the condenser sections (walls and/or floors). The temperature could be easily controlled, providing a comfortable and affordable living environment. Investigating the appropriate materials and working fluids is needed to

determine this application's potential success and usage.

This work was done by Marc Gibson, James Sanzi, and Ivan Locci of Glenn Research Center. Further information is contained in a TSP (see page 1).

Inquiries concerning rights for the commercial use of this invention should be addressed to NASA Glenn Research Center, Innovative Partnerships Office, Attn: Steven Fedor, Mail Stop 4-8, 21000 Brookpark Road, Cleveland, Ohio 44135. Refer to LEW-18900-1.

⚙️ Apparatus for Pumping a Fluid

There are no rotating or moving parts apart from bellows.

Marshall Space Flight Center, Alabama

A fluid pump has been developed for mechanically pumped fluid loops for spacecraft thermal control. Lynntech's technology utilizes a proprietary electrochemically driven pumping mechanism. Conventional rotodynamic and displacement pumps typically do not meet the stringent power and operational reliability requirements of space applications. Lynntech's developmental pump is a highly efficient solid-state pump with essentially no rotating or moving components (apart from metal bellows).

Figure 1 schematically illustrates the electrochemically-driven actuator. The conversion of electrical energy to mechanical work is achieved by transporting hydrogen across an electrochemical cell. Hydrogen is dissociated at the anode; protons that are formed from the dissociation are driven across the membrane by an applied potential, while electrons are conducted through an external circuit; protons and electrons recombine at the cathode to form hydrogen. The transport of hydrogen into and out of the attached bellows results in a pressure variation that is used to actuate the fluid pumping diaphragms. Each electrochemical cell is made up of a proton exchange membrane, typically Nafion®, with platinum catalyzed electrodes on either side, called a membrane electrode assembly (MEA). The use of hydrogen and its low oxidation and reduction potentials results in high electric-to-mechanical work conversion efficiency.

For size and convenience, a plurality of individual MEAs is used to transport the hydrogen, rather than a single electrochemical cell. The MEAs are connected electrically in series and fluidically in parallel. The stack of MEAs is sandwiched between two current collectors, and a voltage is applied across the stack, driving hydrogen gas from one

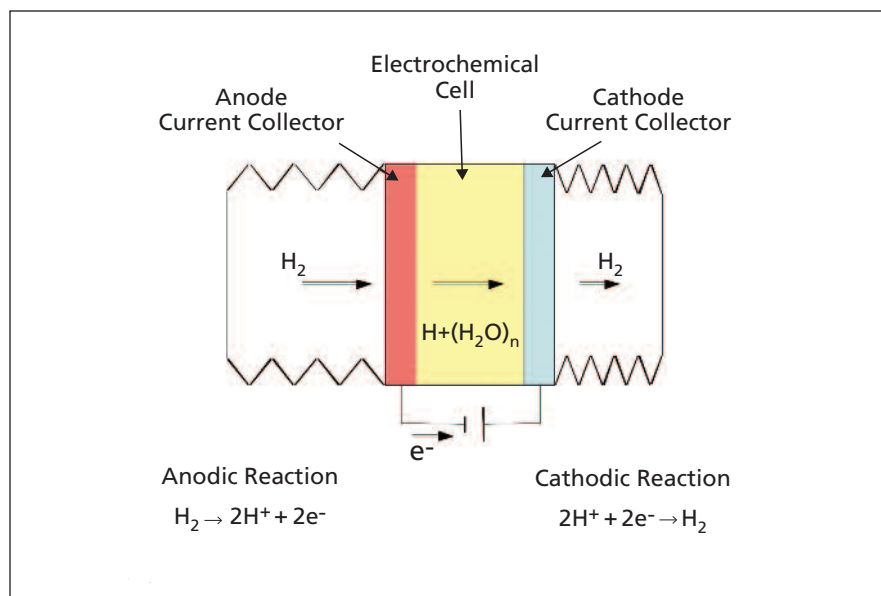


Figure 1. **Hydrogen** is dissociated at the anode; protons formed from the dissociation are conducted through the membrane, while electrons are conducted through an external circuit; protons and electrons recombine at the cathode to form hydrogen.

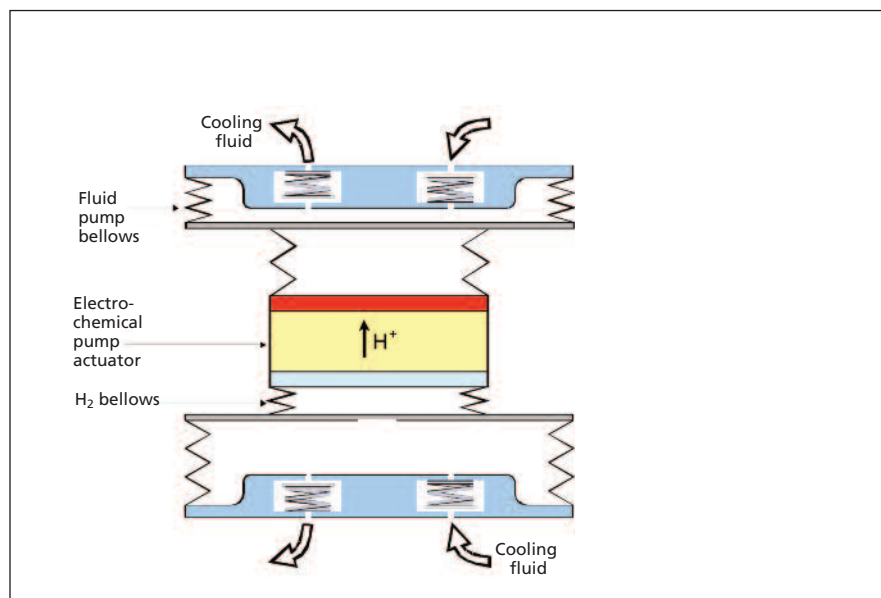


Figure 2. The **Smaller Hydrogen-Filled Bellows** actuates the second larger set of bellows, which displace fluid in the pump heads. Fluid is expelled from one pump head while being drawn into the other.

bellows to the other. The hydrogen flow rate through the actuator is directly proportional to the applied current. The hydrogen-filled bellows are used to actuate a second set of bellows, which displace the fluid in the pump head, as shown schematically in Figure 2. To further reduce the pump power requirements, a stroke-volume multiplier is utilized wherein a smaller-volume hydrogen filled bellows actuates a larger-volume fluid bellows. The stroke volume multiplier also allows the pump frequency to be reduced below audible frequency while maintaining adequate flow.

The largest factor affecting the lifetime and reliability of the pump is expected to be loss of hydrogen from the electrochemical actuator. The electrochemical actuator is hermetically sealed; however, permeation of hydrogen is expected to eventually result in loss of hydrogen. The lifetime of the pump is extended by generating hydrogen onboard the pump. The onboard hydrogen generation also allows the hydrogen pressure and pump performance to be optimized for varying operating temperatures.

The prototype pump is expected to operate with a power consumption of 2.4 W

at a flow rate of 0.76 L/min and pressure rise of 27.6 kPa. The pump will operate at temperatures between 0 and 100 °C and survive temperatures between -60 to 110 °C. The prototype occupies a volume of $\approx 600 \text{ cm}^3$.

This work was done by Robert Van Boeyen and Jonathan Reeh of Lynntech, Inc. for Marshall Space Flight Center. For more information, contact Sammy A. Nabors, MSFC Commercialization Assistance Lead, at Sammy.a.nabors@nasa.gov. Refer to MFS-32760-1.

❁ Cobra Fiber-Optic Positioner Upgrade

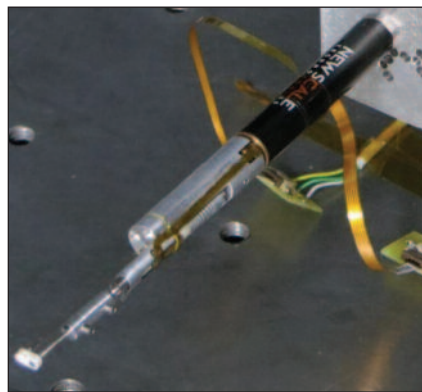
This technology could be used for applications requiring precise location of a small object within a small circular area, such as in medical lasers.

NASA's Jet Propulsion Laboratory, Pasadena, California

A prime focus spectrometer (PFS), along with corrective optics, will mount in place of the secondary mirror of the Subaru telescope on Mauna Kea, Hawaii. This will allow simultaneous observations of cosmologic targets. It will enable large-scale galactic archeology and dark energy surveys to help unlock the secrets of the universe.

To perform these cosmologic surveys, an array of 2,400 optical fibers needs to be independently positioned within the 498-mm-diameter focal plane of the PFS instrument to collect light from galaxies and stars for spectrographic analyses. To allow for independent re-positioning of the fibers, a very small positioner (7.7 mm in diameter) is required. One hundred percent coverage of the focal plane is also required, so these small actuators need to cover a patrol region of 9.5 mm in diameter. To optimize the amount of light that can be collected, the fibers need to be placed within 5 micrometers of their intended target (either a star or galaxy).

The Cobra Fiber Positioner was designed to meet the size and accuracy requirements stated above. Cobra is a two-degrees-of-freedom mechanism that can position an optical fiber in the focal



The Prime Focus Spectrometer (PFS) installed on the Subaru Telescope.

plane of the PFS instrument to a precision of 5 micrometers. It is a theta-phi style positioner containing two rotary piezo tube motors with one offset from the other, which enables the optic fibers to be placed anywhere in a small circular patrol region. The patrol region of the actuator is such that the array of 2,400 positioners allows for full coverage of the instrument focal plane by overlapping the patrol areas.

A second-generation Cobra positioner was designed based on lessons learned from the original prototype

built in 2009. Improvements were made to the precision of the ceramic motor parts, and hard stops were redesigned to minimize friction and prevent jamming. These changes resulted in reducing the number of move iterations required to position the optical fiber within 5 micrometers of its target. At the time of this reporting, there are still many tests to be performed that will validate system level performance, but on an individual level, the Cobra positioner demonstrates excellent performance and will enable the PFS instrument to make unprecedented measurements of the universe.

What is unique about the upgrades made to the Cobra positioner is the improved performance due to the design changes in the hard stops and the ceramic end caps of the motors. Other changes were made to reduce the unit cost of a Cobra positioner without affecting the performance, since thousands of these devices will have to be built for the PFS instrument.

This work was done by Charles D. Fisher, David F. Braun, and Joel V. Kaluzny of Caltech for NASA's Jet Propulsion Laboratory. For more information, contact iaoffice@jpl.nasa.gov. NPO-48751



Improved Wide Operating Temperature Range of Li-Ion Cells

Applications include electric vehicles, where high-energy-density and high-power batteries are needed that can operate at low temperature.

NASA's Jet Propulsion Laboratory, Pasadena, California

Future NASA missions aimed at exploring the Moon, Mars, and the outer planets require rechargeable batteries that can operate over a wide temperature range (-60 to $+60$ °C) to satisfy the requirements of various applications including landers, rovers, penetrators, CEV, CLV, etc. This work addresses the need for robust rechargeable batteries that can operate well over a wide temperature range.

The Department of Energy (DoE) has identified a number of technical barriers associated with the development of Li-ion rechargeable batteries for PHEVs. For this reason, DoE has interest in the development of advanced electrolytes that will improve performance over a wide range of temperatures, and lead to long life characteristics (5,000 cycles over a 10-year life span). There is also interest in improving the high-voltage stability of these candidate electrolyte systems to enable the operation of up to 5 V with high specific energy cathode materials.

Currently, the state-of-the-art lithium-ion system has been demonstrated to operate over a wide range of temperatures (-40 to $+40$ °C); however, the rate capability at the lower temperatures is very poor. In addition, the low-temperature performance typically deteriorates rapidly upon being exposed to high temperatures.

A number of electrolyte formulations were developed that incorporate the use of electrolyte additives to improve the high-temperature resilience, low-tempera-

ture power capability, and life characteristics of methyl propionate (MP)-based electrolyte solutions. These electrolyte additives include mono-fluoroethylene carbonate (FEC), lithium oxalate, vinylene carbonate (VC), and lithium bis(oxalate borate) (LiBOB), which have previously been shown to result in improved high-temperature resilience of all carbonate-based electrolytes. These MP-based electrolytes with additives have been shown to have improved performance in experiments with MCMB-LiNiCoAlO₂ cells.

A number of lithium-ion electrolytes having improved temperature range of operation were demonstrated. LiPF₆-based mixed carbonate electrolyte formulations that contain ester co-solvents have been optimized for operation at low temperature, while still providing reasonable performance at high temperature. In earlier work [see "Optimized Carbonate and Ester-Based Li-Ion Electrolytes" (NPO-44974) *NASA Tech Briefs*, Vol. 32, No. 4 (April 2008), p. 56], ester co-solvents, including methyl propionate (MP), ethyl propionate (EP), methyl butyrate (MB), ethyl butyrate (EB), propyl butyrate (PB), and butyl butyrate (BB), were investigated in multi-component electrolytes of the following composition: 1.0 M LiPF₆ in ethylene carbonate (EC) + ethyl methyl carbonate (EMC) + X (20:60:20 v/v %) [where X = ester co-solvent]. Focusing upon improved rate capability at low temperatures (i.e., -20 to -40 °C), this

approach was optimized further [see "Li-Ion Cells Employing Electrolytes With Methyl Propionate and Ethyl Butyrate Co-Solvents" (NPO-46976), *NASA Tech Briefs*, Vol. 35, No. 10 (October 2011), p. 47], which resulted in the development of 1.20M LiPF₆ in EC+EMC+MP (20:20:60 v/v %) and 1.20M LiPF₆ in EC+EMC+EB (20:20:60 v/v %), which were demonstrated to operate well over a wide temperature range in MCMB-LiNiCoAlO₂ and Li₄Ti₅O₁₂-LiNiCoAlO₂ prototype cells. In the current work, improved high temperature resilience, low temperature power capability, and life characteristics have been provided with methyl propionate-based electrolyte solutions [i.e., 1.20M LiPF₆ in EC+EMC+MP (20:20:60 v/v%)] possessing the additives described above.

This work was done by Marshall C. Smart and Ratnakumar V. Bugga of Caltech for NASA's Jet Propulsion Laboratory. Further information is contained in a TSP (see page 1).

In accordance with Public Law 96-517, the contractor has elected to retain title to this invention. Inquiries concerning rights for its commercial use should be addressed to:

*Innovative Technology Assets Management
JPL*

*Mail Stop 321-123
4800 Oak Grove Drive
Pasadena, CA 91109-8099
E-mail: iaoffice@jpl.nasa.gov*

Refer to NPO-47538, volume and number of this NASA Tech Briefs issue, and the page number.

Non-Toxic, Non-Flammable, -80 °C Phase Change Materials

Lyndon B. Johnson Space Center, Houston, Texas

The objective of this effort was to develop a non-toxic, non-flammable, -80 °C phase change material (PCM) to be used in NASA's ICEPAC capsules for biological sample preserva-

tion in flight to and from Earth orbit. A temperature of about -68 °C or lower is a critical temperature for maintaining stable cell, tissue, and cell fragment storage.

Within this technical effort, two phase change fluids were developed with melting onset at -85 °C and -61 °C, and latent heat of fusion of 100 and 136 J/mL, respectively. The experimental results

indicate good repeatability of the freeze/thaw cycle, compatibility with high-density polyethylene, thermal stability, and flashpoints exceeding 100 °C. Based on the individual components, the phase change fluids are expected to have low acute toxicity.

There are several types of phase change materials (PCMs) that can be considered for the preservation of biological samples at a temperature of about -68 °C. These include hydrated salts in water, non-hydrated or weakly hydrated salts in water, non-electrolyte aqueous solutions, and pure, non-aqueous fluids. However, none of these options resulted

in a -80 °C freezing point stable PCM during the freeze/thaw cycling. Therefore, a non-aqueous mixture was formulated yielding a pseudo melting point plateau, adequate stability over numerous thermal cycles, and suitable latent heats. The product is a non-aqueous base fluid with a somewhat tailored freezing point, and latent heats on the order of 100 J/mL for the -85 °C PCM.

The fluid developed is an organic solution with adequate resistance to biological growth, compatible with HDPE (high density polyethylene) plastic, and is characterized by a negative freezing expansion ratio. The negative

expansion ratio during freezing will allow for the ICEPAC modules to be completely filled with PCM material as compared to previously used fluids requiring a 20-mL air bubble (within a 120-mL capsule). This translates to a 20-percent increase in cooling capacity for a given latent heat. Furthermore, the specific gravity of the PCM is on the order of 0.92 g/mL, making it lighter than an aqueous-based solution per ICEPAC capsule.

This work was done by J. Michael Cutbirth of Mainstream Engineering Corp. for Johnson Space Center. Further information is contained in a TSP (see page 1). MSC-24460-1

Soft-Bake Purification of SWCNTs Produced by Pulsed Laser Vaporization

A more efficient, cost-effective, environmentally friendly method purifies high-quality carbon nanotubes.

Lyndon B. Johnson Space Center, Houston, Texas

The “soft-bake” method is a simple and reliable initial purification step first proposed by researchers at Rice University for single-walled carbon nanotubes (SWCNT) produced by high-pressure carbon monoxide disproportionation (HiPco). Soft-baking consists of annealing as-produced (raw) SWCNT, at low temperatures in humid air, in order to degrade the heavy graphitic shells that surround metal particle impurities. Once these shells are cracked open by the expansion and slow oxidation of the metal particles, the metal impurities can be digested through treatment with hydrochloric acid.

The soft-baking of SWCNT produced by pulsed-laser vaporization (PLV) is not straightforward, because the larger average SWCNT diameters (≈ 1.4 nm) and heavier graphitic shells surrounding metal particles call for increased temperatures during soft-bake. A part of the technology development focused on optimizing the temperature so that effective cracking of the graphitic shells is balanced with maintaining a reasonable yield, which was a critical aspect of this study. Once the ideal temperature was determined, a number of samples of raw SWCNT were purified using the soft-bake method.

An important benefit to this process is the reduced time and effort required for soft-bake versus the standard purification route for SWCNT. The total time

spent purifying samples by soft-bake is one week per batch, which equates to a factor of three reduction in the time required for purification as compared to the standard acid purification method. Reduction of the number of steps also appears to be an important factor in improving reproducibility of yield and purity of SWCNT, as small deviations are likely to get amplified over the course of a complicated multi-step purification process.

The full JSC characterization protocol consisting of UV-Vis-NIR absorption, Raman spectroscopy, thermogravimetric analysis (TGA), scanning electron microscopy (SEM), and transmission electron microscopy (TEM) was applied to all samples. In addition, the nanotube content as the percentage out of total carbon was calculated from UV-Vis-NIR absorption, using a procedure similar to that proposed in earlier research. The nanotube percentage relative to the total sample weight was calculated from the absorption data, taking into account the metal content. These measurements were used to quantify various aspects of the “quality” of the material in terms of: metal content (TGA residue weight percentage), oxidation temperature (the temperature of the most significant peak in the first derivative of the TGA), stability of DMF dispersion by optical absorption, nanotube content (weight percentage of total from UV-

Vis-NIR absorption and TGA), the frequency of the Raman G-band peak, and the ratio between the D-band and G-band intensities. All measurements (except dispersion stability) were repeated three times to determine variability of the purification route through statistical methods. Standard deviations of the experimental results are considered important parameters to quantify the homogeneity of nanotube samples.

The data indicate that the major properties, such as metal content, nanotube content, oxidation temperature, and extent of defects as determined by Raman, are similar or superior for the soft-baked samples when compared to the standard acid-purified samples. TGA and Raman data suggest that there is more metal removed, less oxidative damage, less protonation, and less derivatization incurred from the acid treatment in soft-baked samples. The stability and reproducibility of DMF dispersions is also superior, suggesting that soft-baking leads to greater homogeneity in materials than standard acid purification routes.

The observed improvement in efficiency translates directly into greater yield and quality of nanotubes, reduced cost and processing time, and the use of lesser amounts of organic solvents and concentrated acids, making the process safer and more environmentally friendly. This approach, as

well as the development of a quality control, may be useful in the industrial scale-up of production and purification of carbon nanotubes.

This work was done by Leonard Yowell of Johnson Space Center, and Pavel Nikolaev, Olga Gorelik, Rama Kumar Allada, Edward Sosa, and Sivaram Arepalli of ERC, Inc. Fur-

ther information is contained in a TSP (see page 1). MSC-24379-1



Improved Cell Culture Method for Growing Contracting Skeletal Muscle Models

This method has great potential for biomedical research and medical treatment.

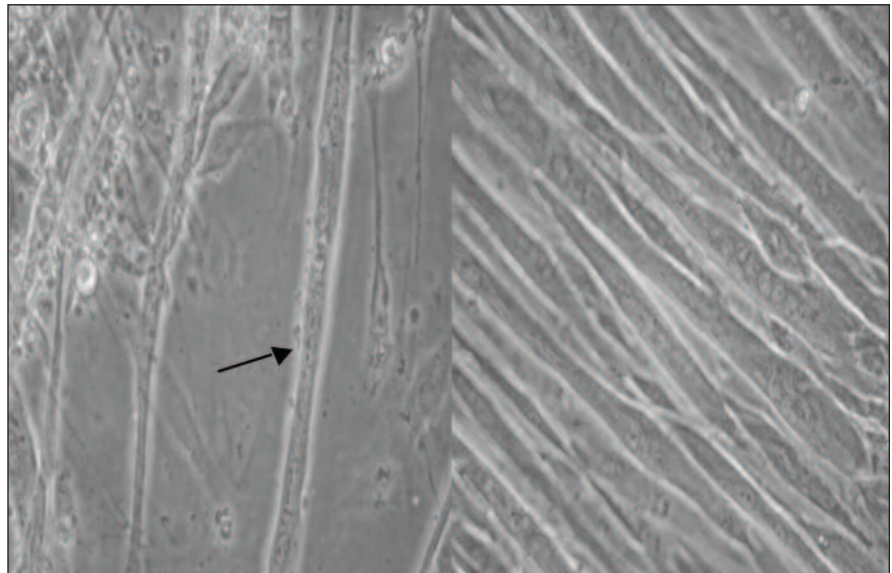
Lyndon B. Johnson Space Center, Houston, Texas

An improved method for culturing immature muscle cells (myoblasts) into a mature skeletal muscle overcomes some of the notable limitations of prior culture methods. The development of the method is a major advance in tissue engineering in that, for the first time, a cell-based model spontaneously fuses and differentiates into masses of highly aligned, contracting myotubes. This method enables (1) the construction of improved two-dimensional (monolayer) skeletal muscle test beds; (2) development of contracting three-dimensional tissue models; and (3) improved transplantable tissues for biomedical and regenerative medicine applications. With adaptation, this method also offers potential application for production of other tissue types (i.e., bone and cardiac) from corresponding precursor cells.

In order to form or repair skeletal muscle tissue, myoblasts must proliferate, align, fuse to form myotubes (maturing, elongated, multinucleated cells), and differentiate to produce new proteins necessary for contraction. Heretofore, none of the typical culture methods has enabled the growth of skeletal muscle tissue possessing all of these characteristics. Notable limitations of prior methodologies include:

- Differentiation is usually induced by the use of undefined serum switches or deprivation, either of which can result in decreased cell viability, occasional unpredictable variations, and experimental bias.
- Alignment of cells is affected by means of time-consuming procedures that involve the use of expensive, complex, micropatterned substrates.
- Spontaneous contraction is a random, rare event.

In contrast, the present method enables the generation of large numbers of aligned, spontaneously contracting myotubes without the use of serum switches or special substrates. The resources necessary for practicing this method are readily available in most cell-culture lab-



Comparison of Skeletal Muscle Culture Methods: Typical culture using serum switches results in random distribution of myotubes (left). The arrow indicates one of many myotubes in the image. The improved cell culture methodology produces aligned myotubes (right) without the use of (micropatterned) substrate modification.

oratories.

The method is embodied in a cost-effective, multistep protocol of cell culture that results in the formation of the desired skeletal muscle tissue model and that, with additional time in culture, yields sheets of spontaneously contracting aligned muscle cells. Omitting most details for the sake of brevity, the protocol is summarized as follows:

1. From typical cell culture of the desired cell type, the cells are removed and concentrated. The cells are resuspended in culture medium to achieve a specific cell density.
2. Cells are seeded onto the bottoms of tissue culture Petri dishes.
3. New culture medium is added to the dish and cultured at 37 °C. After 3 days of incubation, myotubes are evident. At 5 to 6 days, myotubes are aligned and are in greater abundance.
4. From this point onward, Petri dishes should be monitored on a daily basis and medium should be replaced with culture medium on an as-needed basis.

5. By the end of a two-week culture period, spontaneously contracting myotubes are evident although contractions may have been noted as early as day 5.

6. Contracting myotubes can be maintained for an additional two weeks with daily culture medium replacement. During this additional culture time, sheets of aligned contracting myotubes appear to gain synchronicity.

The theory underlying this methodology includes the following elements:

- Low-density cell culture favors cell flattening. Flattened cell morphology, in the presence of growth factors found in the culture medium, encourages cell proliferation. In this new methodology, the lower-density cell population will also proliferate. The newly formed cells, crowded by adjacent newly formed cells, are forced to compete for attachment space and are forced to align.
- Simultaneously, the cell crowding caused by the high-density cell population prevents total cell flattening. In-

stead, the attached, rounded morphology, coupled with the high degree and duration of cell-to-cell contact, is thought to induce expression of genes that causes the cells to switch from proliferating to differentiating phenotype. This differentiating phenotype gains the ability to fuse and express contractile proteins.

Currently, this model can serve as an improved, yet easily generated, in vitro skeletal muscle test bed for evaluating signal transduction pathways, stretch activated ion channels, protein synthesis regulation, and interactions with the ex-

tracellular matrix and membrane proteins with the cytoskeleton. The ease and low cost of generation makes this model a valuable option to many laboratories that have the desire, but lack the sophisticated resources previously required to explore the mechanisms of muscle atrophy. Future development of the model into a three-dimensional construct provides a potential powerful tool for defining the mechanisms of microgravity-induced muscle atrophy, identification of molecular targets for novel countermeasure development, and testing of some countermeasures.

This work was done by Michele L. Marquette of the University of Texas Medical Branch, and Marguerite A. Sognier of the Universities Space Research Association for Johnson Space Center. For further information, contact the JSC Innovation Partnerships Office at (281) 483-3809.

This invention is owned by NASA, and a patent application has been filed. Inquiries concerning nonexclusive or exclusive license for its commercial development should be addressed to the Patent Counsel, Johnson Space Center, (281) 483-1003. Refer to MSC-24314-1

Hand-Based Biometric Analysis

Goddard Space Flight Center, Greenbelt, Maryland

Hand-based biometric analysis systems and techniques provide robust hand-based identification and verification. An image of a hand is obtained, which is then segmented into a palm region and separate finger regions. Acquisition of the image is performed without requiring particular orientation or placement restrictions. Segmentation is performed without the use of reference points on

the images. Each segment is analyzed by calculating a set of Zernike moment descriptors for the segment.

The feature parameters thus obtained are then fused and compared to stored sets of descriptors in enrollment templates to arrive at an identity decision. By using Zernike moments, and through additional manipulation, the biometric analysis is invariant to rotation, scale, or translation or an input

image. Additionally, the analysis uses re-use of commonly seen terms in Zernike calculations to achieve additional efficiencies over traditional Zernike moment calculation.

This work was done by George Bebis of University of Nevada, Reno for Goddard Space Flight Center. For further information, contact the Goddard Innovative Partnerships Office at (301) 286-5810. GSC-16141-1

The Next Generation of Cold Immersion Dry Suit Design Evolution for Hypothermia Prevention

The system design recovers warm exhaled air and re-circulates it inside the suit.

John H. Glenn Research Center, Cleveland, Ohio

A body at sea is vulnerable to hypothermia, which often leads to loss of life. Hypothermia is caused by the differences between the core body temperature and the surrounding air and seawater temperatures. The greater the differences between the body core temperature and the sea temperature, the more rapidly the core body temperature will drop, and hypothermia can quickly set in. Heat loss is primarily caused by conduction of heat away from the body. Most cold immersion suits on the market are passive designs that only insulate the body against the cold, although some cold immersion suits use special materials such as paraffin to absorb heat and to radiate the heat back to the body. This new utility patent is an active design that relies on the lung's role as an organic heat ex-

changer for providing deep body core heating of air. It is based on the fact that the greatest heat loss mechanism for an insulated human body immersed in a cold water environment is due to heat loss through respiration.

This innovation successfully merges two existing technologies (cold immersion suit and existing valve technologies) to produce a new product that helps prevent against the onset of hypothermia at sea. During normal operations, a human maintains an approximate body temperature of [98.6 °F (37 °C)]. A mechanism was developed to recover the warm temperature from the body and reticulate it in a survival suit. The primary intention is to develop an encompassing systems design that can both easily and cost effectively be integrated in all existing currently manufac-

ture cold water survival suits, and as such, it should be noted that the cold water immersion suit is only used as a framework or tool for laying out the required design elements.

At the heart of the suit is the Warm Air Recovery (WAR) system, which relies on a single, large Main Purge Valve (MPV) and secondary Purge Valves (PV) to operate. The main purge valve has a thin membrane, which is normally closed, and acts as a one-way check valve. When warm air is expelled from the lungs, it causes the main purge valve to open. Air forced from the MPV is dumped directly into the suit, thereby providing warmth to the torso, legs, and arms. A slight positive over-pressure in the suit causes warm waste air (or water if the suit is punctured) to be safely vented into the sea through large PVs located at the bot-

tom of each arm and leg. The secondary purge valves act to prevent the buildup of large concentrations of CO₂ gas and help guard against asphyxia. It is noted that the MPV causes the inhalation and exhalation cycles to be completely isolated from one another in the current suit design.

The main problem with the existing survival suit designs stems from cold sea water entering the suit through the gaps around the face opening in the hood and inflatable neck collar. Cold water entering the suit is caused by high wind and waves, a problem that is further exacerbated if the suit is submerged by a wave. The problem is easily solved using four integral components: an optically transparent full face shield, a nose/mouth mask, a Surface Air Valve (SAV), and a MPV.

Surface air valve integration with the suit is effected by affixing the SAV on the outward side of the face shield with a short tube extending through the face shield, which is directly plumbed to the air inlet port on the mask. WAR system integration with the suit is achieved by connecting the MPV to the air outlet port located at the bottom of the mask near the mouth.

A special type of SAV mechanism called a Pressure Release Valve (PRV) is employed in the current design. When the PRV is above the sea surface, the PRV is open, allowing the lungs to in-

hale a fresh atmospheric air. The PRV automatically closes when submerged. This PRV has the advantage of being able to operate in any position, even while completely submerged upside down. The PRV is connected to a short tube extending through the face shield, and the open end of the tube is terminated with yet another purge valve located at the air inlet port on the mask. The PRV and PV combo results in a unique new type of valve called a Pressure Release/Purge valve (PR/P) that is designed to compensate for additional heat loss from the respiration cycle and only applies to situations when the PR/P valve is above the sea surface. The following two examples are considered:

Example (1) is a situation in which the air inlet port on the mask is connected to the PRV by a short tube extending through the face shield. Since the PRV is above the sea surface, the PRV is open and air can freely be drawn into the lungs. When warm air is exhaled from the lungs, it causes air to flow outward through the PRV, causing the body to lose valuable heat during the exhalation cycle. Therefore, in this example, the inhalation and exhalation cycles are no longer separated from one another.

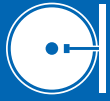
Example (2) is a situation in which the PR/P valve on the face shield is connected to the air inlet port on the mask, and the MPV is connected to the air out-

let port on the mask. Because the PR/P valve is above the sea surface, the PR/P valve is open. The action of drawing air from the mask causes the PV located at the end of the PR/P valve to open and the MPV to close. When air is exhaled from the lungs into the mask, it causes the PV located on the end of the PR/P valve to close, and warm exhaled air flowing into the mask forces the MPV to open, venting warm air directly into the suit. Thus the PR/P valve recovers any heat loss during the exhalation part of the respiration cycle.

The new technology represents a substantial improvement over existing state-of-the-art survival suit designs and should greatly extend the length of time a body can survive in hazardous cold-water conditions encountered in the North Atlantic, Bering Sea, and other cold regions of the world. This suit technology is intended to be utilized by the various branches of the U.S. Coast Guard, the U.S. Navy, the Merchant Marine, as well as the commercial fishing industry fleet.

This work was done by Joel Galofaro of Glenn Research Center. Further information is contained in a TSP (see page 1).

Inquiries concerning rights for the commercial use of this invention should be addressed to NASA Glenn Research Center, Innovative Partnerships Office, Attn: Steven Fedor, Mail Stop 4-8, 21000 Brookpark Road, Cleveland, Ohio 44135. Refer to LEW-18960-1.



Integrated Lunar Information Architecture for Decision Support Version 3.0 (ILIADS 3.0)

ILIADS 3.0 provides the data management capabilities to access CxP-vetted lunar data sets from the LMMP-provided Data Portal and the LMMP-provided On-Moon lunar data product server. (LMMP stands for Lunar Mapping and Modeling Project.) It also provides specific quantitative analysis functions to meet the stated LMMP Level 3 functional and performance requirements specifications that were approved by the CxP.

ILIADS 3.0 is a rich client (aka, thick client) lunar Geospatial Information System (GIS) software application. It is a redesigned software framework and architecture that leverages GSFCs experience developing the ILIADS 2.0 core software. Specifically, ILIADS 3.0 is built upon ILIADS 2.0.

The purpose of ILIADS 3.0 is to provide an integrated, rich client lunar GIS software application. Most significantly, the objective in designing and developing ILIADS 3.0 was to provide a flexible and expandable software framework that readily enabled new features and functions to be integrated into ILIADS driven by the science and engineering user community. To contribute to the decision support process, ILIADS 3.0 also provides interfaces to readily enable interoperability between ILIADS 3.0 and other NASA-developed lunar information systems whenever it may become required to interface ILIADS with such systems.

By building upon Goddard's IRC core framework, ILIADS is also well suited to being readily integrated with future lunar surface system assets (e.g., crewed rovers, spacesuits) as an embedded system application. ILIADS 3.0 provides cross-platform support and thus executes on a diverse suite of computing platforms that are used by NASA scientists and engineers. The application is designed to provide authorized/authenticated users with the ability to use the Internet to securely, yet easily, identify and locate geographically distributed sources of vetted lunar data products that have been derived from US and international lunar spacecraft missions. It can query the data catalogs

of these sources to identify available lunar data products and the metadata associated with them. The software uses standard OGC (Open Geospatial Consortium) WMS, WCS, and WFS (Web Map Service, Web Coverage Service, and Web Feature Service) services to access mapped lunar delta products from these sources so that they may be processed by ILIADS 3.0 and rendered as multiple semi-transparent raster or vector visualizations, so that the lunar data product information is readily understood in the context of one another.

This work was done by Stephen Talabac, Troy Ames, Karin Blank, Carl Hostetter, and Matthew Brandt of Goddard Space Flight Center. Further information is contained in a TSP (see page 1). GSC-16210-1

Relay Forward-Link File Management Services (MaROS Phase 2)

This software provides the service-level functionality to manage the delivery of files from a lander mission repository to an orbiter mission repository for eventual spacelink relay by the orbiter asset on a specific communications pass. It provides further functions to deliver and track a set of mission-defined messages detailing lander authorization instructions and orbiter data delivery state. All of the information concerning these transactions is persisted in a database providing a high level of accountability of the forward-link relay process.

This is an improvement over legacy processes that required lander client users to log into orbiter mission workstations and run orbiter-specific applications. The legacy process provided only a simple e-mail indicating success of transaction, and no further accounting of the forward-link transaction.

The Phase 2 MaROS forward-file management functions represent a significant upgrade of this relay system. This version provides a lander team the capability of selecting a set of "forward-link" files to be radiated to an orbiter for relay during a chosen communications window. These forward-link files contain critical flight data such as spacecraft command sequences and flight software uploads; this new MaROS functionality is classified Class

B software. This new software version also includes the capability for lander and orbiter team members to associate predefined messages to the chosen set of forward-link files. Lander teams can specify authorizations for the orbiter team such as "go for radiation," and orbiter team members may specify status messages such as "onboard spacecraft." All of the status data is tracked in a database and provided via a shared service interface. The system provides a high level of accountability into the forward-link process.

This work was done by Daniel A. Allard, Michael N. Wallick, Franklin H. Hy, and Roy E. Gladden of Caltech for NASA's Jet Propulsion Laboratory. Further information is contained in a TSP (see page 1).

This software is available for commercial licensing. Please contact Dan Broderick at daniel.f.broderick@jpl.nasa.gov. Refer to NPO-47942.

Two Mechanisms to Avoid Control Conflicts Resulting from Uncoordinated Intent

This software implements a real-time access control protocol that is intended to make all connected users aware of the presence of other connected users, and which of them is currently in control of the system. Here, "in control" means that a single user is authorized and enabled to issue instructions to the system.

The software also implements a goal scheduling mechanism that can detect situations where plans for the operation of a target system proposed by different users overlap and interact in conflicting ways. In such situations, the system can either simply report the conflict (rejecting one goal or the entire plan), or reschedule the goals in a way that does not conflict.

The access control mechanism (and associated control protocol) is unique. Other access control mechanisms are generally intended to authenticate users, or exclude unauthorized access. This software does neither, and would likely depend on having some other mechanism to support those requirements.

This work was done by Andrew H. Mishkin, Daniel L. Dvorak, David A. Wagner, and Matthew B. Bennett of Caltech for NASA's Jet Propulsion Laboratory. Further information is contained in a TSP (see page 1).

This software is available for commercial licensing. Please contact Dan Broderick at daniel.f.broderick@jpl.nasa.gov. Refer to NPO-47732.

XTCE GOVSAT Tool Suite 1.0

The XTCE GOVSAT software suite contains three tools: validation, search, and reporting. The Extensible Markup Language (XML) Telemetric and Command Exchange (XTCE) GOVSAT Tool Suite is written in Java for manipulating

XTCE XML files. XTCE is a Consultative Committee for Space Data Systems (CCSDS) and Object Management Group (OMG) specification for describing the format and information in telemetry and command packet streams. These descriptions are files that are used to configure real-time telemetry and command systems for mission operations. XTCE's purpose is to exchange database information between different systems.

XTCE GOVSAT consists of rules for narrowing the use of XTCE for missions.

The Validation Tool is used to syntax check GOVSAT XML files. The Search Tool is used to search (i.e. command and telemetry mnemonics) the GOVSAT XML files and view the results. Finally, the Reporting Tool is used to create command and telemetry reports. These reports can be displayed or printed for use by the operations team.

This work was done by J. Kevin Rice of Global Science & Technology, Inc. for Goddard Space Flight Center. Further information is contained in a TSP (see page 1). GSC-16279-1



▶ Determining Temperature Differential to Prevent Hardware Cross-Contamination in a Vacuum Chamber

Goddard Space Flight Center, Greenbelt, Maryland

When contamination-sensitive hardware must be tested in a thermal vacuum chamber, cross-contamination from other hardware present in the chamber, or residue from previous tests, becomes a concern. Typical mitigation strategies involve maintaining the temperature of the critical item above that of other hardware elements at the end of the test.

A formula for relating the pumping speed of a chamber, the surface area of contamination sources, and the temperatures of the chamber, source, and con-

tamination-sensitive items has been developed. The formula allows the determination of a temperature threshold about which contamination will not condense on the sensitive items. It defines a parameter alpha that is the fraction given by (contaminant source area)/[chamber pumping speed × (time under vacuum)^{0.5}]. If this parameter is less than 10⁻⁶, cross-contamination from common spacecraft material will not occur when the sensitive hardware is at the same temperature as the source of contamination (The chamber is isothermal within 5

°C.).

Knowing when it becomes safe to have the hardware isothermal permits faster and easier thermal transitions when compared with maintaining an arbitrary temperature differential between parts. Furthermore, the standard temperature differential may not be adequate under some conditions ($\alpha > 10^{-4}$).

This work was done by David Hughes of Goddard Space Flight Center. For further information, contact the Goddard Innovative Partnerships Office at (301) 286-5810. GSC-16244-1

▶ SequenceL: Automated Parallel Algorithms Derived from CSP-NT Computational Laws

Chip manufacturers and developers of parallel and/or safety-critical software could benefit from this innovation.

Goddard Space Flight Center, Greenbelt, Maryland

With the introduction of new parallel architectures like the cell and multicore chips from IBM, Intel, AMD, and ARM, as well as the petascale processing available for high-end computing, a larger number of programmers will need to write parallel codes. Adding the parallel control structure to the sequence, selection, and iterative control constructs increases the complexity of code development, which often results in increased development costs and decreased reliability.

SequenceL is a high-level programming language — that is, a programming language that is closer to a human's way of thinking than to a machine's. Historically, high-level languages have resulted in decreased development costs and increased reliability, at the expense of performance. In recent applications at JSC and in industry, SequenceL has demonstrated the usual advantages of high-level programming in terms of low cost and high reliability.

SequenceL programs, however, have run at speeds typically comparable with, and in many cases faster than, their counterparts written in C and C++ when run on single-core processors. Moreover, SequenceL is able to generate parallel executables automatically for multicore hardware, gaining parallel speedups without any extra effort from the programmer beyond what is required to write the sequential/single-core code.

A SequenceL-to-C++ translator has been developed that automatically renders readable multithreaded C++ from a combination of a SequenceL program and sample data input. The SequenceL language is based on two fundamental computational laws, Consume-Simplify- Produce (CSP) and Normalize-Transpose (NT), which enable it to automate the creation of parallel algorithms from high-level code that has no annotations of parallelism whatsoever. In our anecdotal experience, SequenceL development has been in every case less costly

than development of the same algorithm in sequential (that is, single-core, single process) C or C++, and an order of magnitude less costly than development of comparable parallel code. Moreover, SequenceL not only automatically parallelizes the code, but since it is based on CSP-NT, it is provably race free, thus eliminating the largest quality challenge the parallelized software developer faces.

Compiling functional code to C++ is not new. Compiling functional code to readable C++ that runs in parallel is much more of a challenge, and that was the majority of this effort. For current purposes in this effort, readability of the generated code is crucial, in case the human programmer wishes to add annotations, or to inspect the code for verification purposes. Moreover, by compiling to C++ it is assured that SequenceL can be used in any application where C++ could be used.

SequenceL has been found to discover all potential parallelisms automat-

ically in relatively complex algorithms (involving multiple threads), and thus shows the potential to relieve more of the programmer's cognitive load as the problem grows in complexity. Sequen-

ceL's runtime environment then selects which parallelisms to actually exploit, with the aim of maximum overall speed when considering communication costs between processes.

This work was done by Daniel Cooke and J. Nelson Rushton of Texas Tech University for Goddard Space Flight Center. Further information is contained in a TSP (see page 1). GSC-15859-1

➤ Remote Data Exploration with the Interactive Data Language (IDL)

Goddard Space Flight Center, Greenbelt, Maryland

A difficulty for many NASA researchers is that often the data to analyze is located remotely from the scientist and the data is too large to transfer for local analysis. Researchers have developed the Data Access Protocol (DAP) for accessing remote data. Presently one can use DAP from within IDL, but the IDL-DAP interface is both limited and cumbersome. A more powerful and user-friendly interface to DAP for IDL has been developed.

Users are able to browse remote data sets graphically, select partial data to retrieve, import that data and make customized plots, and have an interactive

IDL command line session simultaneous with the remote visualization. All of these IDL-DAP tools are usable easily and seamlessly for any IDL user.

IDL and DAP are both widely used in science, but were not easily used together. The IDL DAP bindings were incomplete and had numerous bugs that prevented their serious use. For example, the existing bindings did not read DAP Grid data, which is the organization of nearly all NASA datasets currently served via DAP.

This project uniquely provides a fully featured, user-friendly interface to DAP

from IDL, both from the command line and a GUI application. The DAP Explorer GUI application makes browsing a dataset more user-friendly, while also providing the capability to run user-defined functions on specified data. Methods for running remote functions on the DAP server were investigated, and a technique for accomplishing this task was decided upon.

This work was done by Michael Galloy of Tech-X Corporation for Goddard Space Flight Center. Further information is contained in a TSP (see page 1). GSC-16021-1

➤ Mixture-Tuned, Clutter Matched Filter for Remote Detection of Subpixel Spectral Signals

NASA's Jet Propulsion Laboratory, Pasadena, California

Mapping localized spectral features in large images demands sensitive and robust detection algorithms. Two aspects of large images that can harm matched-filter detection performance are addressed simultaneously. First, multimodal backgrounds may thwart the typical Gaussian model. Second, outlier features can trigger false detections from large projections onto the target vector.

Two state-of-the-art approaches are combined that independently address outlier false positives and multimodal backgrounds. The background clustering of Funk et al. models multimodal backgrounds, and the mixture tuned matched filter (MT-MF) of Boardman

et al. addresses outliers. Combining the two methods captures significant additional performance benefits. The resulting mixture tuned clutter matched filter (MT-CMF) shows effective performance on simulated and airborne datasets.

The classical MNF transform was applied, followed by k-means clustering. Then, each cluster's mean, covariance, and the corresponding eigenvalues were estimated. This yields a cluster-specific matched filter estimate as well as a cluster-specific feasibility score to flag outlier false positives.

The technology described is a proof of concept that may be employed in fu-

ture target detection and mapping applications for remote imaging spectrometers. It is of most direct relevance to JPL proposals for airborne and orbital hyperspectral instruments. Applications include subpixel target detection in hyperspectral scenes for military surveillance. Earth science applications include mineralogical mapping, species discrimination for ecosystem health monitoring, and land use classification.

This work was done by David R. Thompson, Lukas Mandrake, and Robert O. Green of Caltech for NASA's Jet Propulsion Laboratory. For more information, contact iaoffice@jpl.nasa.gov. NPO-48663



Partitioned-Interval Quantum Optical Communications Receiver

The receiver structure described here improves upon the performance of optical communications links, achieving high sensitivity and high data rates even with extremely weak optical signals.

NASA's Jet Propulsion Laboratory, Pasadena, California

The proposed quantum receiver in this innovation partitions each binary signal interval into two unequal segments: a short "pre-measurement" segment in the beginning of the symbol interval used to make an initial guess with better probability than 50/50 guessing, and a much longer segment used to make the high-sensitivity signal detection via field-cancellation and photon-counting detection. It was found that by assigning as little as 10% of the total signal energy to the pre-measurement segment, the initial 50/50 guess can be improved to about 70/30, using the best available measurements such as classical coherent or "optimized Kennedy" detection.

However, 70% detection probability (or, equivalently, 30% error probability) is not good enough for communications, even with the most powerful codes, which require error probabilities in the 0.01–0.1 range to achieve the desired coded performance. Due to the requirement to maintain a constant-envelope local laser field, the recently

reported "optimized Kennedy" measurement was selected for making this initial guess. The outcome of this first measurement is used to decide which signal the receiver should try to null. Hence, the local field envelope and phase are adjusted to nearly cancel the more likely signal, and photon counting is used for the rest of the interval to confirm this initial decision. If the wrong signal is selected initially, then the local laser adds instead of subtracting a constant matched laser field to the received signal, yielding a higher probability error; that is, higher probability of erroneously pre-selecting the "other" binary signal. Optimum partitioning of the signal interval is critical, and must be carried out for each new value of K_s . This concept can be extended directly to more than two intervals, by partitioning the first interval itself into two segments, optimized for the smaller initial energy, to further improve the "pre-measurement" upon which the final high-sensitivity measurement strategy is based.

The performance gain of the partitioned-interval quantum receiver over the well-known Kennedy receiver detection strategy is shown in Figure 2, along with the gains of the classical coherent receiver and the optimized Kennedy receiver. It is noted that the coherent receiver peaks at an average received photon-count of $K_s = 0.095$ attaining a maximum gain of 1.272 over the Kennedy receiver, whereas the optimized Kennedy receiver peaks at $K_s = 0.165$, with a maximum gain of 1.381, after which both gains decrease as the average signal energy increases: the optimized Kennedy receiver approaches 1 at high signal energies, reverting back to the conventional Kennedy receiver, whereas the coherent receiver continues towards zero. However, the partitioned-interval receiver described here attains higher gains, and tends to maintain these gains near their maximum value even with increasing signal energy.

The only receiver structure known to achieve the quantum limit theoretically

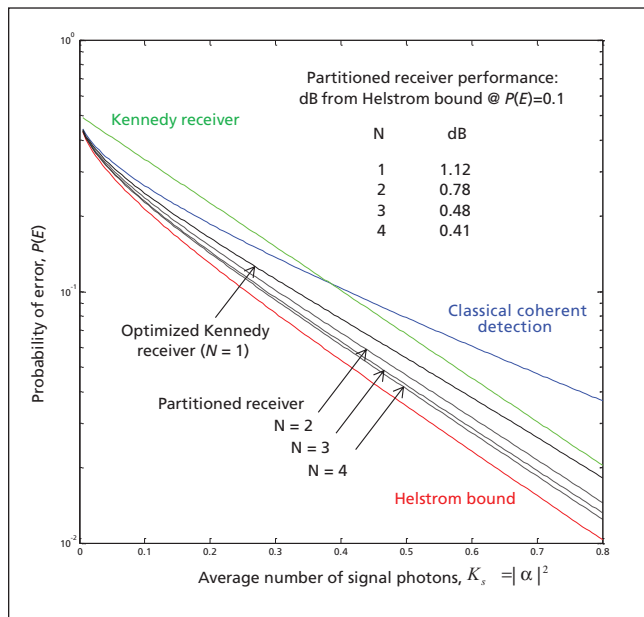


Figure 1. Error Probability Performance and comparison of N -segment partitioned receivers.

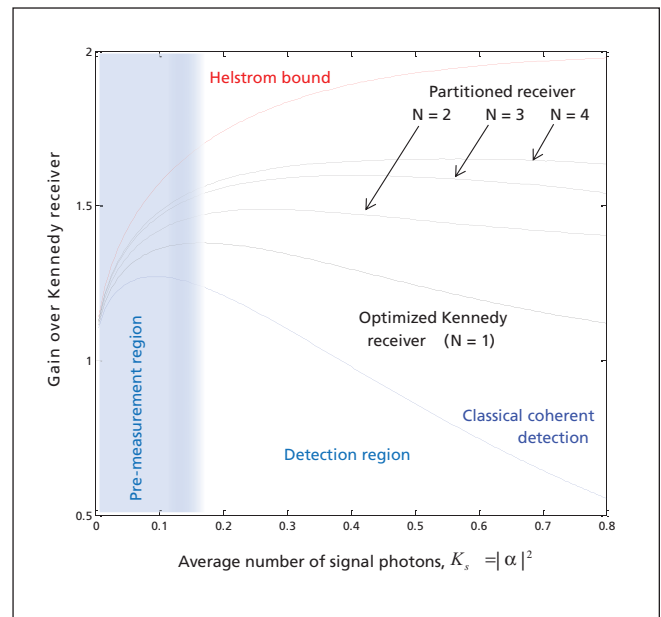


Figure 2. Gain of Coherent, Optimized Kennedy and partitioned receivers over Kennedy receiver.

on binary signal detection (the curves labeled “Helstrom bound” in Figures 1 and 2) is known as the Dolinar receiver. This approach applies a rapidly time-varying local laser field to the signal during each bit-interval, but such time-varying fields are difficult to generate in practice at high data rates. In addition, the phase and sign of the local laser fields must be switched instantaneously with the detection of each new photon for best performance, placing significant burdens on the processing speed of the receiver and on the response of the local laser. The proposed solution over-

comes these problems by employing constant local laser intensities that can be pre-computed based on estimates of signal-strength, while attaining nearly the same bit-error rate as the more complex quantum-optimum receiver. The solution proposed here will therefore enable high-sensitivity deep-space optical communications at data rates up to gigabits/second as required for future deep-space optical communications.

This work was done by Victor A. Vilnrotter of Caltech for NASA’s Jet Propulsion Laboratory. For more information, contact iaoffice@jpl.nasa.gov.

In accordance with Public Law 96-517, the contractor has elected to retain title to this invention. Inquiries concerning rights for its commercial use should be addressed to:

*Innovative Technology Assets Management
JPL*

Mail Stop 321-123

4800 Oak Grove Drive

Pasadena, CA 91109-8099

E-mail: iaoffice@jpl.nasa.gov

Refer to NPO-48496, volume and number of this NASA Tech Briefs issue, and the page number.

Practical UAV Optical Sensor Bench With Minimal Adjustability

Goddard Space Flight Center, Greenbelt, Maryland

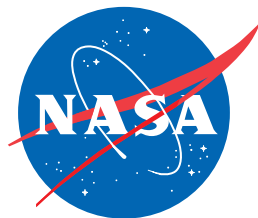
A multiple-pass optical platform eliminates essentially all optical alignment degrees of freedom, save one. A four-pass absorption spectrometer architecture is made rigid by firmly mounting dielectric-coated mirror prisms with no alignment capability to the platform. The laser diode beam is collimated by a small, custom-developed lens, which has only a rotational degree of freedom along the standard optical “z” axis. This degree is itself eliminated by adhesive after laser collimation. Only one degree of freedom is preserved by allowing the laser diode chip and mount subassembly to move relative to the collimating lens

by using over-sized mounting holes. This allows full 360° motion of a few millimeters relative to the lens, which, due to the high numerical aperture of the lens, provides wide directional steering of the collimated laser beam.

Because the optical layout has been designed to provide proper mirror alignment for an orthonormal, paraxial laser beam, this degree of freedom is sufficient to insure perfect optical alignment once the orthonormal condition is satisfied. Further, the degree of freedom is enabled by using either simple loose metal screws in the over-sized laser mounting holes, plastic screws with low

tension, or a combination of the two. Once alignment is achieved, the screws are tightened sufficiently to insure ruggedness, or the plastic screws may be replaced, one by one, with metal screws. In either case, even the remaining degree of freedom is locked down after the final alignment. The final degree of freedom may be permanently, or quasi-permanently, locked by use of various adhesives on the screw head or threads.

This work was done by Jeffrey Pilgrim and Paula Gonzales of Vista Photonics, Inc. for Goddard Space Flight Center. Further information is contained in a TSP (see page 1). GSC-16536-1



National Aeronautics and
Space Administration